Successive multilayer desorption from ultrathin alkali-metal films studied with helium-atom scattering

D. Fuhrmann, E. Hulpke, and W. Steinhögl
Max-Planck-Institut für Strömungsforschung, D-37073 Göttingen, Germany
(Received 2 June 1997; revised manuscript received 29 August 1997)

Using high-resolution energy-resolved helium-atom scattering the temperature-dependent behavior of phonons in ultrathin potassium films has been investigated. The experiments show that ''organ pipe'' modes with frequencies determined by the local film thickness dominate the phonon dispersion curves in films of thicknesses below ten monolayers. The vanishing of certain film modes and the emergence of new modes at sufficiently high temperatures indicates a partial and, eventually, a complete thermal desorption of the film. An evaluation of the data demonstrates that the desorption proceeds in a layer-by-layer mode. At temperatures below the onset of desorption annealing effects have been measured, also using the spectroscopy of different film modes. [S0163-1829(98)04807-3]

I. INTRODUCTION

The most common techniques applied in desorption spectroscopy involve thermal or electronic excitation of the system and the detection of changes in the surface coverage or the desorbed particle flux.[1,2] In this paper a method is introduced that allows one to study the desorption behavior of ultrathin films and provides more detailed information than conventional thermal desorption spectroscopy (TDS). In contrast to conventional TDS, changes in the distribution of confined vibrational modes in the film,[3–5] measured in the energy transfer spectra of scattered He atoms, are used to monitor the local film thickness and thus the coverage Θ. In this way additional information on the desorption process can be obtained and also, possibly, on the difference between the kinetic parameters for films of different thicknesses.

In this paper we present helium-atom scattering (HAS) data for the K/Ni(001) system. Following a section about the details of the experiment, three different aspects of the results will be discussed. First, it will be shown how the diffuse elastic component of the scattered helium provides insight into the onset of desorption from the film surfaces. Then the measured intensities of the confined vibrational (''organ pipe'') modes in the energy transfer spectra of the scattered helium will be presented. As a third aspect the influence of the temperature on the distribution of film modes in the energy transfer spectra will be discussed as well as how the behavior of the data can be used as an identifying characteristic to gain information on the morphology of the film surfaces and on the annealing process. The last two sections are devoted to the description of a model that is quantitatively able to explain the data and provides values for the activation energies for desorption from films of different thicknesses.

II. EXPERIMENTAL DETAILS

The HAS apparatus used in the experiments is described in detail elsewhere.[6] It employs time-of-flight (TOF) spectroscopy with an energy transfer resolution corresponding to 350 μeV at a beam energy of 12.4 meV. All TOF spectra in this paper have been converted to an energy transfer scale. The Ni(001) substrate (Kristallhandel Kelpin, D-69181 Leimen) was cleaned by repeated cycles of sputtering with 800-eV Ar^+ followed by an annealing procedure at 1100 K until Auger electron spectroscopy indicated that the sulfur and carbon contamination is below the detection limit of the instrument [$\Theta < 0.5\%$ of a monolayer (ML)]. Potassium getter dispensers (SAES getters S.P.A., Milano, Italy), mounted 60 mm away from the substrate, were used to deposit the alkali-metal films. Before use the dispensers were carefully outgassed and before each experiment they were heated for 1 h to a temperature slightly below the operating conditions. The oscillations in the specularly reflected He signal during alkali-metal deposition served to determine the film thickness[7–9] in terms of the number of deposited alkali-metal ML's. On ceasing the exposure at the Nth maximum one obtains a film of N-ML ''nominal'' thickness.

The surface temperature was measured with a chromel-alumel thermocouple welded to the crystal. The thermocouple readings were calibrated *in situ*[10] by measuring the desorption of different adsorbed atoms and molecules [K,[11] CO,[12] and N_2 (Ref. 13)]. In each one of these adsorbate systems the onset of desorption was indicated by a sudden increase in the specular reflectivity on raising the temperature. In this manner, the temperatures for peaks in the desorption spectra of these systems have been determined and compared to TDS data from the literature.[11–13] Computer controlled heating made it possible to achieve a stability of the surface temperature of $\pm$ 0.6 K and also permits the temperature to be raised linearly with time. Heating rates were chosen to be on the order of 0.1 K/s. Measurements of the angular shift of the specular He reflection for different temperatures indicated that in the temperature range between 100 K and 350 K misalignments of the crystal caused by thermal expansion in the crystal holder assembly were smaller than 0.05° and can be neglected.

III. RESULTS

A. Thermal desorption

The helium data show that thermal desorption from ultrathin ($\Theta < 10$ ML) potassium films on a Ni(001) substrate

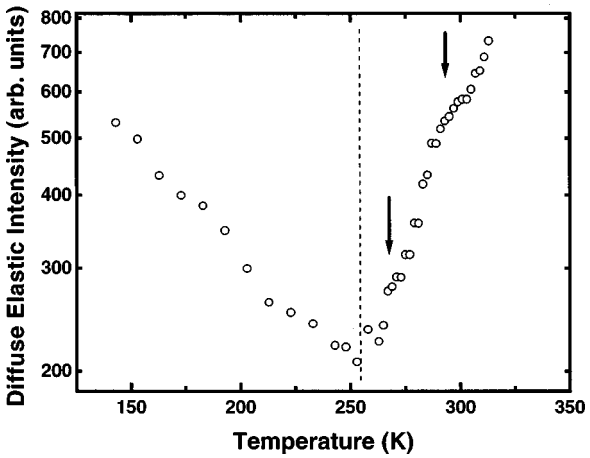

FIG. 1. Temperature evolution of the ''diffuse elastic'' peak intensity measured in the He energy transfer spectra at a parallel momentum transfer of $\Delta K = 0.35$ Å^{-1}, at 12.0 meV beam energy, and along the [110] azimuth direction of the Ni(001) substrate. The sample was prepared by depositing 4 ML of potassium on the substrate at 98 K at a rate of 0.1 ML/sec. Raising the temperature leads initially to a Debye-Waller damping of the signal and later to an increase in the concentration of surface defects due to the desorption of K atoms. The temperature that marks the onset of desorption is indicated by the dashed line, the arrows indicate temperatures at which the desorption from islands with 4 and 5 ML thickness is completed (see the text).

leads to drastic changes in the surface morphology. Thus the onset of desorption can be detected by monitoring the ''diffuse elastic'' peak in the TOF spectra of the scattered He as the film temperature is raised since this peak contains helium atoms that are elastically scattered by defects on the surface.[14,15]

Figure 1 illustrates how the diffuse elastic peak intensity changes on increasing the surface temperature. The particular set of data refers to a potassium film prepared to be 4 ML thick using the criterion described above. It had been deposited at 100 K substrate temperature and had not been annealed. The intensities plotted are taken from a series of energy transfer spectra measured at different temperatures for a parallel momentum transfer of $\Delta K = 0.35$ Å^{-1} along the [110] substrate azimuth for an incident beam energy of 12 meV. The semilogarithmic presentation shows that, at sufficiently low temperatures, the intensity decreases with increasing temperature. Such a behavior and the linear slope of the curve are expected and are due to Debye-Waller attenuation.[16] For temperatures larger than 260 K the diffuse elastic intensity rises again rapidly. This indicates that the Debye-Waller attenuation has been superseded by an enhancement of the diffuse intensity brought about by an increasing number of surface defects, which are most likely due to the onset of desorption. Thus the temperature at which desorption from the K-film surface becomes significant lies substantially below 336 K, the melting point of bulk potassium.[17] It is also interesting to note that the rising part of the curve in Fig. 1 contains additional structure at 270 K and 290 K, marked by arrows in the plot. An evaluation of changes in the distribution of film modes discussed in Sec. III C reveals that this structure is due to a layer-by-layer desorption mechanism and the marked temperatures are related to completing the removal of another monolayer.

B. Film modes

Using TOF spectroscopy, changes in the phonon spectrum of the ultrathin potassium films with temperature have been investigated. As for the Na/Cu(001) film system[3,4] the TOF spectra measured for K films on Ni(001) up to 10 ML thickness contain peaks related to vibrational modes representing confined resonances within the potassium layer.[18,19] These standing longitudinal waves exhibit nodes at the film-substrate interface and antinodes at the film surface and result in a vibrational mode at the surface with a polarization vector parallel to its normal that warrants a large excitation probability for inelastic helium scattering.[20] The frequency of these modes is directly related to the thickness of the film and thus to the number of monolayers N deposited on the substrate. Since the wavelengths of the overtones are odd integer multiples of that of the fundamental frequency $\omega_1(N)$, it has become customary to label these modes by $1/N, 3/N, \ldots$.[3,21] A comparison of such film modes for a variety of systems[4] has revealed that, for $N \geqslant 2$, the fundamental frequency $\omega_1(N)$ can be written as

$$\omega_1(N) = \omega_0 N^{-p}, \tag{1}$$

where ω_0 and p are parameters that are characteristic of the film-substrate combination. It turns out that for Na/Cu(001), $p = 1$, in which case Eq. (1) describes the fundamental frequencies of the vibrations in an organ pipe. In the K/Ni(001) system the exponent p has the value of 1.23 and $\hbar\omega_0 = 13.12$ meV.[19]

The nature of these vibrations implies that the resonance frequencies measured in a HAS experiment should be independent of the amount of parallel momentum ΔK transferred to the surface and thus of scattering geometry or beam energy. Earlier experiments for the K/Ni(001) system confirm this behavior as long as the film thickness and the momenta transferred are sufficiently small and the ''dispersion curves'' for the 1/3, 1/4, and 1/5 modes are perfectly ''flat'' for $\Delta K \leqslant 0.3$ Å^{-1}.[19]

The aim of the investigation in this paper is to take advantage of the unambiguous relation between film mode frequencies and the film thickness from Eq. (1) and to use it as an identifying characteristic to monitor temperature-induced changes in the film. In order to rule out systematic errors that are caused by an undesired variation in experimental parameters, great care was taken to avoid the misalignment of the crystal due to thermal expansion in the crystal holder assembly ($\leqslant 0.05°$). The influence of the temperature-dependent multiphonon excitation was kept as small as possible by operating at a very low helium beam energy of 12 meV.

Figure 2 shows a helium TOF spectrum, converted to an energy transfer scale, that was obtained from a film of a ''nominal'' thickness of 4 ML at a fixed incident angle $\theta_i = 47.5°$ and at 12.0 meV beam energy. The potassium film was deposited at 100 K substrate temperature and at a rate of 0.1 ML/s while monitoring the specular He reflectivity. The desired nominal thickness was obtained as described earlier. After the potassium atom flux was turned off the temperature was raised to 148 K and the TOF spectrum shown in Fig. 2

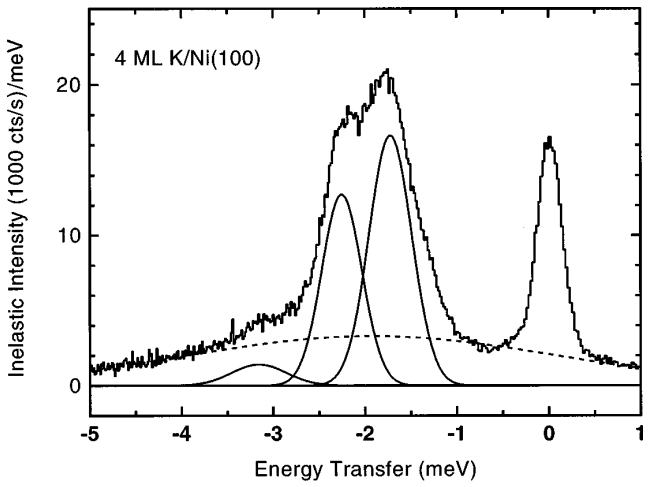

FIG. 2. Helium energy transfer spectrum, measured under the experimental conditions stated in the legend of Fig. 1, after the temperature was raised to 148 K. The deconvolution of the spectrum reveals contributions of the 1/5 film mode at -1.8 meV, the 1/4 mode at -2.3 meV, and the 1/3 mode at -3.3 meV. The diffuse elastic peak is seen at $\Delta E = 0$ meV.

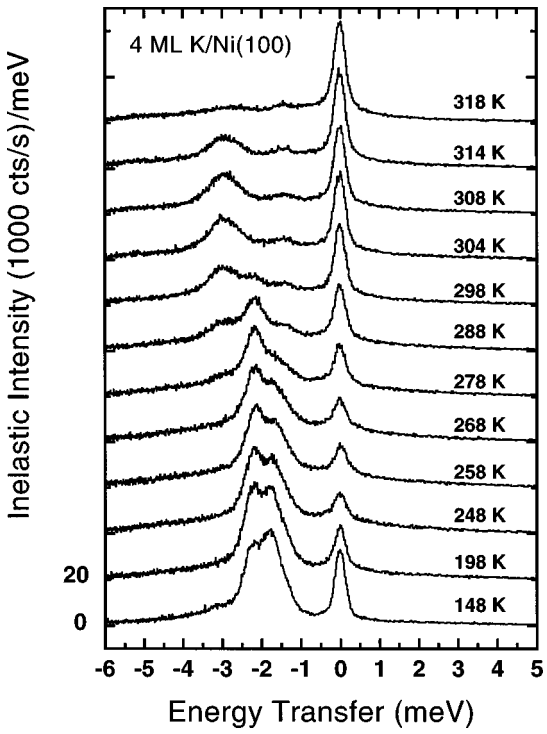

FIG. 3. Evolution of He energy transfer spectra as the sample temperature is raised. The other experimental parameters are the same as in the legend of Fig. 1. The different peaks can be assigned to the diffuse elastic peak at 0 meV, the Rayleigh wave of the Ni substrate at -1.7 meV, the 1/5 film mode at -1.8 meV, the 1/4 film mode at -2.3 meV, the Rayleigh wave of the substrate for different kinematic conditions at -2.4 meV, and the 1/3 film mode at -3.3 meV. Further experiments show that the sequence becomes irreversible on lowering the temperature again.

was measured. It contains in addition to the diffuse elastic peak at $\Delta E = 0$ some structure that can be fitted using three Gaussian profiles on top of a broad Gaussian representing the contribution of multiphonon excitations.[22] The deconvolution was performed using the program PEAKFIT, version 4.0, supplied by Jandel Scientific Software, in which the centers, the widths, and the amplitudes of the four Gaussians are adjusted simultaneously such that an optimum fit to the data is achieved. It turns out that the three phonon inelastic peaks in Fig. 2 are located at -1.8 meV, -2.3 meV, and -3.3 meV. A comparison with the results presented in Ref. 19 shows that these vibrational energies are precisely those of the confined resonances 1/5, 1/4, and 1/3, indicating that the film investigated is not of uniform thickness: While the largest contribution to the energy transfer spectrum in Fig. 2 is due to a confined resonance in a 4-ML-thick film, modes related to a local thickness of 5 ML and 3 ML are also observed.

C. Temperature effects

The sequence of traces in Fig. 3 illustrates the evolution of the data presented in Fig. 2 when the temperature is raised. If the film temperature is increased by ΔT and the TOF measurements are repeated on the same film without changing the scattering geometry or the beam energy, the energy transfer spectrum is observed to change considerably. Not only is the diffuse elastic intensity reduced due to the Debye-Waller attenuation discussed above, but the amplitudes of the three different contributions to the structured peak in the bottom trace (the data shown in Fig. 2) also change and, at sufficiently high temperatures, new signatures appear in the spectra until, at temperatures above 318 K, the excitation of the Rayleigh wave of the clean Ni substrate dominates. All of these temperature-induced changes in the film were found to be irreversible: While at lower temperatures changes in the spectra reflect the annealing process, at higher temperatures a layer-by-layer desorption takes place. Lowering the sample temperature again in several steps from 320 K to 290 K does not change the appearance of the TOF spectra[23] aside from Debye-Waller effect induced changes in the intensities of the three peaks displayed in the trace for 318 K in Fig. 3. The spectrum at 318 K contains a particularly large diffuse elastic peak suggesting a considerable number of randomly distributed defects that are probably K atoms in a low submonolayer concentration. Obviously, the desorption was not completed at this temperature, an assumption that agrees with adsorption studies of the related K/Cu(001) system. They show that even at a temperature of 373 K some potassium atoms remain adsorbed on the surface.[24]

In very satisfying agreement with the previous work on the K films,[19] the following assignment can be given to the peaks seen in Fig. 3: The diffuse elastic peak appears at 0 meV, the Rayleigh wave of the Ni substrate at -1.7 meV, the 1/5 film mode at -1.8 meV, the 1/4 film mode at -2.3 meV, the Rayleigh wave of the substrate for different kinematic conditions at -2.4 meV, and the 1/3 film mode at -3.3 meV.

Figure 3 contains just samples of the complete sequence of TOF spectra measured. In Fig. 4. the intensities of the different film modes, which were extracted from these data by the Gauss-profile fitting procedure discussed above, are plotted as a function of temperature. It is straightforward to understand the behavior of the curves in a qualitative way: At the lowest temperatures the presence of three film modes indicates that the unannealed film consists of patches that are

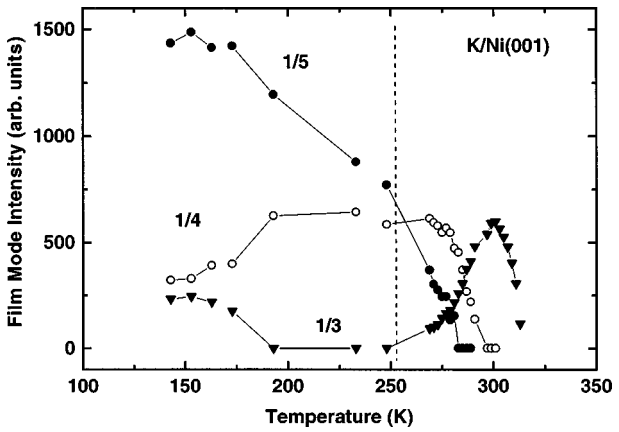

FIG. 4. Layer-by-layer ''desorption spectra'' from a 4-ML potassium film. Shown are changes in the film mode intensities in the He energy transfer spectra as a function of the film temperature. The intensities correspond to the area of the individual peaks extracted from the data in Fig. 3 using the deconvolution scheme discussed in the text: 1/5 mode, filled circles; 1/4 mode, open circles; 1/3 mode, triangles. At lower temperatures annealing effects dominate the temperature dependence, at higher ones successive ablation of the 5-ML, 4-ML, and 3-ML patches on the film is observed. As in Fig. 1, the dashed line marks the onset of desorption-induced surface roughening.

3, 4, and 5 ML thick. On raising the temperature up to ≈ 260 K the 3-ML patches are being filled up by interlayer diffusion of atoms from the 5-ML and 4-ML patches and the area of the 4-ML islands increases accordingly. The number and size of these islands increases further at the onset of desorption from the surface of 5-ML patches occurring at ≈ 245 K. At ≈ 270 K atoms from the surface of 4-ML patches desorb, exposing again the 3-ML-thick film underneath. At ≈ 300 K the 1/5 and 1/4 modes have disappeared, indicating that the film has now reached a uniform thickness of 3 ML. Above this temperature the 3-ML patches are being depleted.

IV. EVALUATION OF THE DATA

Gaining quantitative information on the desorption process from the temperature programmed desorption spectra depicted in Fig. 4 turns out to be a difficult task. There are a number of effects that make it cumbersome to relate the inelastic peak intensities to the surface dynamics.

The shape of the curves in Fig. 4 is brought about by the combination of two processes, interlayer diffusion between patches of different thickness and, at sufficiently high temperatures, desorption from the patch surfaces. Both processes determine the evolution of the patch sizes with temperature as it is raised linearly with time. The intensities of inelastic peaks in the energy transfer spectra, subsequently called film mode intensities for short, are related to the total surface area covered with patches of the respective size. The first problem one has to deal with is the fact that this relationship itself depends on the average patch size that determines whether the inelastic signal from different patches results from a *coherent* or an *incoherent* superposition of the scattered de Broglie waves.

Another problem arises because the film mode intensities contain an extra temperature dependence due to the Bose factor[22] and the Debye-Waller-factor[25] that enter the formula describing the inelastic reflection probability.[26] In addition, the intensities of the film modes are attenuated by the competition with diffuse elastic scattering, which, in the systems studied here, also displays a strong temperature dependence (cf. Fig. 1).

The following subsections deal with these different aspects. In Sec. IV A the dependence of the film mode intensities on the area covered with patches of different thicknesses will be discussed. Section IV B describes how the influence of the temperature on the intensities due to the Bose and Debye-Waller factors will be taken into account. Section IV C finally introduces a kinetic model that is used to describe the dynamics and to reproduce the measured temperature behavior of the different film mode intensities. The calculated curves will be corrected for the influence of the competing diffuse elastic scattering. In this model we will restrict ourselves to describe the behavior for temperatures above 263 K and assume that in this range interlayer diffusion is completed due to the relatively small activation energy of only 40 meV (Ref. 19) and the relatively long time interval of 6300 s that has elapsed between the measured spectra at 148 K and at 263 K.

A. Inelastic intensity and patch area

Depending on the transfer width of the apparatus[27] and the size of patches of a certain thickness, the inelastically scattered de Broglie waves contribute in different ways to the film mode intensities. If two adjacent patches of different thickness cover a sufficiently large area, an *incoherent* superposition of the inelastic contributions has to be considered and the relative film mode intensities are proportional to the surface area of these patches. The transfer width of the helium spectrometer used in the experiment is 210 Å at a beam energy of 12 meV. Measurements of changes in the specular intensity profile for the Ni(001) sample, which was used as a substrate, indicate that the average lateral terrace size was somewhat smaller than 200 Å (Ref. 23) and it is reasonable to assume that patches of a certain thickness are even smaller in size. Furthermore, in the course of the desorption process the patches will shrink in size. In this case, however, the *coherent* superposition of the different inelastically scattered waves must be taken into account.

In order to understand the dependence of the film mode intensity on the island size for a coherent superposition it will be assumed that the film consists of two patches, one $N+1$ ML thick, covering an area Θ_{N+1}, and another one N ML thick, covering the remaining substrate area Θ_N. The wave function Ψ of the coherent inelastically scattered helium can be decomposed into two parts, each one proportional to the respective areas the He atoms had interacted with:

$$\Psi = \Psi_{N+1}\Theta_{N+1} + \Psi_N\Theta_N . \tag{2}$$

The first term on the right-hand side carries information on the excitation of film modes in the patch that is $N+1$ ML thick, the second one on the excitation of those in the patch that is N ML thick. If the total area is normalized to unity $\Theta_N + \Theta_{N+1} = 1$, the scattered intensity I can be written as

$$I=|\Psi_{N+1}|^2(1-\Theta_N)^2+|\Psi_N|^2\Theta_N^2+(\Psi_{N+1}^*\Psi_N+\Psi_N^*\Psi_{N+1})\times(1-\Theta_N)\Theta_N. \quad (3)$$

The last part of the sum contains products of wave functions with different frequency factors because they have been scattered from areas with different film thickness and have suffered different energy gains or losses. Therefore, the frequency factors in the mixed terms do not cancel out and their time average is zero. Thus, in general, the film mode intensity is proportional to the square of the corresponding area for a coherent superposition of the scattered waves.

In the case that $\Theta_N^2 \ll 1$ Eq. (2) can be approximated by

$$I=(1-2\Theta_N)|\Psi_{N+1}|^2+\Theta_N^2|\Psi_N|^2, \quad (4)$$

where the intensity of the $1/(N+1)$ mode in the He energy transfer spectra is determined by the first term and that of the $1/N$ mode by the second. In this formula the influence of defects on the scattered signal is neglected.

Equation (4) predicts that if the area of the thinner patch, Θ_N, is increased by removing atoms from the thicker layer into the gas phase, the peak intensity of the $1/N$ mode will grow in proportion to Θ_N^2. At the same time the film mode signal related to the film that is being depleted decreases linearly in Θ_N.

B. Correcting for other temperature effects

If the film mode intensities are to be used to get information on the evolution of the surface morphology as the temperature is changed with time, the temperature dependence of the film mode intensities due to the Bose and Debye-Waller factors must be taken into account. The Bose factor,[26] which contains just the phonon frequency and the temperature as parameters, can be calculated for the respective experimental conditions and the data in Fig. 4 can be corrected easily for its influence. However, corrections of film mode intensities for the Debye-Waller effect require an additional effort. It has been previously discovered that the Debye temperature of alkali-metal films depends strongly on the film thickness.[19] In a separate experiment the Debye-Waller factors for well annealed films of nominal thicknesses of 3, 4, and 5 ML have been determined by measuring the specular He atom reflectivity from the film surfaces as a function of temperature. It was found that the Debye temperature extracted from the data according to Eq. (45) in Ref. 25 amounts to 157 K for 3-ML-thick, 130 K for 4-ML-thick, and 123 K for 5-ML-thick films (see also Ref. 19). Using these results, the influence of the Debye-Waller effect on the intensities of the 1/5, 1/4, and 1/3 modes in Fig. 4 can be divided out.

In general, both corrections should distinctly modify the shape of the curves plotted in Fig. 4. The restriction to temperatures above 226 K mentioned earlier reduces this influence and, due to the small range of temperatures involved, the combination of both corrections leads to a mere scaling of the curves by constant factors of 2.3, 2.2, and 1.3 for the 1/5, 1/4, and 1/3 branches, respectively. The third correction for temperature-dependent effects, in which the competing diffuse elastic scattering is taken into account, will be applied to the results of the calculations introduced in the following subsection.

C. Successive layer-by-layer desorption

In the kinetic model, which is used to provide a quantitative description, of the layer-by layer desorption, it is assumed that the film consists of three different patches, one being 5 ML thick and covering a substrate area Θ_5, a second one 4 ML thick and covering an area Θ_4, and a 3-ML patch on an area Θ_3. As mentioned before, we will restrict ourselves to temperatures above 263 K and assume that in this range interlayer diffusion is completed due to the relatively small activation energy of only 40 meV.[19] With the further assumption of first-order desorption kinetics and that desorption occurs in a layer-by-layer mode, one arrives at the following three coupled differential equations that govern the time evolution of the areas covered by the patches of different thickness and thus of the film mode intensities:

$$\frac{d\Theta_5}{dt}=-k_5\Theta_5,$$

$$\frac{d\Theta_4}{dt}=-k_4\Theta_4+k_5\Theta_5,$$

$$\frac{d\Theta_3}{dt}=-k_3\Theta_3+k_4\Theta_4, \quad (5)$$

where Θ_n is the area of the respective patch of $n=5, 4$, and 3 ML thickness and k_n the related desorption rate constant that follows Arrhenius's law

$$k_n=\nu\exp-\frac{E_n}{k_BT}, \quad (6)$$

with ν denoting the statistical preexponential, E_n the activation energy for desorption, and k_B the Boltzmann constant. It has turned out to be necessary and even essential to assume that E_n is different for patches of different thickness in order to reproduce the experimentally observed time evolution of the film mode intensities.

Figure 5 illustrates how the solutions of the coupled differential equations compare with the data. For this purpose the data shown in Fig. 4 for temperatures above 263 K have been corrected for the Bose and Debye-Waller factors as discussed above. In this range the temperature T was changed linearly with time t as

$$T(t)\ (\mathrm{K})=263+4.25\times10^{-3}t\ (\mathrm{s}). \quad (7)$$

Thus the desorption rate constants in Eq. (4) become functions of time. After taking this time dependence into account the coupled differential equations are solved numerically for the boundary conditions given by the values of the respective experimental data at $T=263$ K or $t=0$. In Fig. 5 the corrected data are plotted such that the temperature scale in Fig. 4 has been converted into a time scale according to Eq. (5). Also plotted are the calculated film mode intensities $I_n(t)$ $(n=5,4,3)$ versus the time, which are assumed to be given by

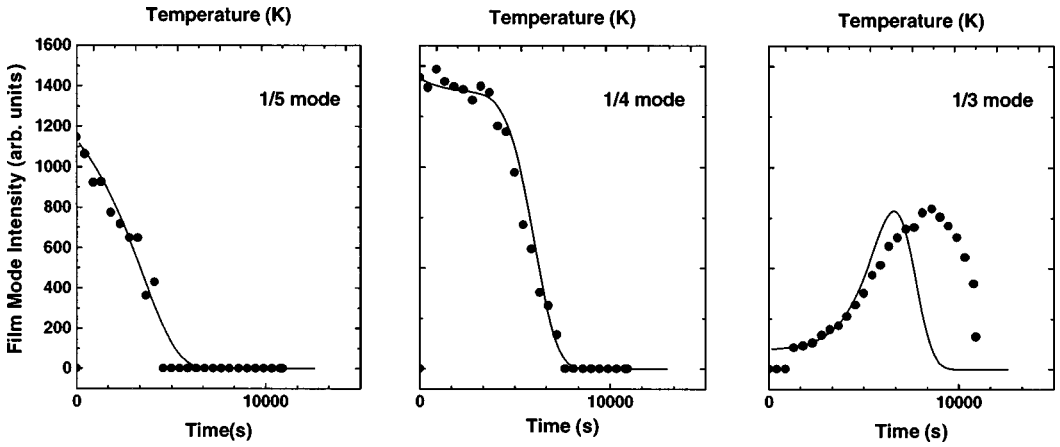

FIG. 5. Comparison of measured and calculated film mode intensities as a function of time for a temperature ramp that is linear in time. The data shown as symbols are the ones presented in Fig. 4 for temperatures above 263 K that have been corrected for the influence of the Bose and Debye-Waller factors (see the text). They refer to a K film grown on Ni(001) at a substrate temperature of 98 K. The ''nominal'' film thickness amounts to 4 ML. The calculations yield activation energies for desorption that depend on the thickness of the respective patches contributing to the surface morphology of the film. Theoretical results are shown as solid lines and have been obtained by assuming first-order desorption kinetics and the set of kinetic parameters given in the text.

$$I_n(t)=[\Theta_n(t)]^2[1-cI_{\text{diffuse}}(T(t))], \tag{8}$$

where $\Theta_n(t)$ are the solutions of Eq. (3) for $n=5, 4$, and 3 and c is an adjustable parameter that takes into account the amount of intensity damping due to diffuse elastic scattering. I_{diffuse} represents the measured diffuse elastic intensity shown in Fig. 1 in which the temperature scale has been converted to a time scale again. Thus the model contains five parameters, the pre-exponential ν and the activation energies E_n $(n=3,4,5)$ from Eq. (4), as well as the number c.

D. Results of the calculations and discussion

With the assumption that the pre-exponential is determined by the largest phonon frequency in bulk K, which amounts to $\nu=$ 2.35 THz,[28] the remaining four parameters were adjusted to achieve a good fit to the experimental data. As mentioned before, it was essential to assume that E_3 is different from E_4 and E_5. The solid line curves shown in Fig. 5 are solutions of Eq. (3) for the set of parameters $E_5=885$ meV, $E_4=900$ meV, $E_3=912$ meV, and $c=1\times10^{-4}$, which reproduces the shape of the experimental curves, in particular those for $n=5$ and 4, reasonably well. The activation energies are in good agreement with the desorption energy evaluated in Ref. 11 for the ''multilayer'' desorption peak (866 meV) with the assumption of $\nu=10$ THz.

The boundaries within which these adjusted parameters may be varied turn out to be fairly narrow: Neglecting the effect of diffuse elastic scattering $(c=0)$ or assuming $c>1.7\times10^{-4}$ makes it impossible to achieve a satisfactory fit for any set of activation energies. The variation of c between 1×10^{-4} and 1.7×10^{-4} can be compensated by changes in E_4 of about 1% and in E_3 of 5%. If one allows for deviations of the fit from the data of $\pm10\%$ each one of the E_n may not be changed by more than $\pm1\%$.

A definite shortcoming of the fitting scheme presented here as compared to the conventional TDS is that the positions and the shapes of the desorption peaks give no direct information on the activation energies from the associated temperatures or on the order of the desorption kinetics from the peak symmetry. We have assumed, in accordance with Ref. 11, the desorption to be of first order because, to our knowledge, there is no work in the literature that suggests deviations from monomer desorption of K atoms.

It is in the nature of multiparameter fitting problems that often the ''best-fit'' parameters are not unique. If no restrictions are put on the value of the the pre-exponential, a better fit to the 1/3 mode data can be achieved, however, at the expense of the quality of the fit to the data for the other modes. The model described above has been extended by introducing additional terms to Eq. (5) that account for desorption from the borders of the respective patches of different thickness with possibly different activation energies. In spite of these additional adjustable parameters it was not possible to obtain a better fit to the data, in particular to that of the 1/3 mode. Furthermore, the assumption of 1/2 order or second-order desorption kinetics or considering an incoherent superposition of inelastic contributions does not improve this situation: Neither one leads to changes in the values for the activation energies by more than 1% for the fixed pre-exponential of 2.35 THz.

V. SUMMARY AND CONCLUSIONS

High-resolution inelastic helium scattering turns out to be a very useful tool in molecular-beam epitaxy. While the elastic component provides information on the growth mode and the thickness of the film,[9] it is shown in this work that the distribution of different confined vibrational film modes in the energy transfer spectra is an identifying characteristic for the distribution of patches of different local film thickness. This technique can be used to characterize the morphology of the film surface. Since these film modes are a phenomenon that is not restricted to alkali-metal films,[4,5] it is applicable to sufficiently thin films of any substance. Changes in the inelastic peak intensities related to the excitation of the film modes with temperature allow one to monitor the annealing process and to explore the conditions under which

annealing results in a film of uniform thickness.

Partial and finally complete desorption of the film can also be investigated with inelastic helium scattering. The actual strength of the technique introduced in this paper lies in the possibility to simultaneously detect desorption from islands of different thickness and to identify the contributions of desorption from each individual patch by using the characteristic information of the respective film mode. In the case of the ''soft'' potassium metal films it is found from the evolution of the film mode intensities that the desorption proceeds in a layer-by-layer fashion.

The scattering process is extremely sensitive to the concentration of defects on the surface. In the system studied here, desorption is accompanied by surface roughening and thus by an increase in the concentration of defects. Therefore, it was possible to use HAS measurements to determine the onset of desorption.

The time evolution of the film mode intensities during desorption has been modeled assuming first-order desorption kinetics and accounting for the attenuation due to the temperature-dependent diffuse elastic scattering. In order to achieve agreement with the data it turns out to be necessary to introduce activation energies for desorption that depend on the film thickness. Assuming an attempt frequency $\nu = 2.35$ THz, equal to the highest phonon frequency in bulk potassium, one obtains values for the activation energies for desorption of $E_5 = 885$ meV, $E_4 = 900$ meV, and $E_3 = 912$ meV. These numbers compare reasonably well with values found in a conventional TDS experiment from potassium films of a sufficiently large thickness [$E_a = 866$ meV (Ref. 11)].

ACKNOWLEDGMENTS

We thank Professor J. P. Toennies for stimulating discussions. We are also grateful to Professor J. R. Manson for helping us to understand the inelastic reflection coefficients and to Dr. P. Bagus and Dr. A. Graham for carefully reading the manuscript and for their helpful criticism.

[1] See, e.g., D. Menzel, in *Chemistry and Physics of Solid Surfaces*, edited by R. Vanselow and R. Howe (Springer, Berlin, 1982).
[2] H. Schlichting and D. Menzel, Surf. Sci. **272**, 27 (1992).
[3] G. Benedek, J. Ellis, A. Reichmuth, P. Ruggerone, H. Schief, and J.P. Toennies, Phys. Rev. Lett. **69**, 2951 (1992).
[4] N.S. Luo, P. Ruggerone, J.P. Toennies, G. Benedek, and V. Celli, J. Electron Spectrosc. Relat. Phenom. **64/65**, 755 (1993).
[5] N.S. Luo, P. Ruggerone, and J.P. Toennies, Phys. Rev. B **54**, 5051 (1996).
[6] H.-J. Ernst, E. Hulpke, and J.P. Toennies, Phys. Rev. B **46**, 16 081 (1992).
[7] J.J. de Miguel, A. Cebollada, J.M. Gallego, J. Ferrón, and S. Ferrer, J. Cryst. Growth **88**, 442 (1988).
[8] B.J. Hinch, C. Koziol, J.P. Toennies, and G. Zhang, Europhys. Lett. **10**, 341 (1989).
[9] G. Rosenfeld, R. Servaty, Ch. Teichert, B. Poelsema, and G. Comsa, Phys. Rev. Lett. **71**, 895 (1993).
[10] H. Schlichting and D. Menzel, Rev. Sci. Instrum. **64**, 2013 (1993).
[11] Y.-M. Sun, H.S. Luftman, and J.M. White, Surf. Sci. **139**, 379 (1984).
[12] N. Vasquez, Jr., A. Muscat, R.J. Madix, Surf. Sci. **301**, 83 (1994).
[13] M. Golze, M. Grunze, and W. Unertl, Prog. Surf. Sci. **22**, 101 (1986).
[14] A.M. Lahee, J.R. Manson, J.P. Toennies, and Ch. Wöll, Phys. Rev. Lett. **57**, 471 (1986).
[15] A.M. Lahee, J.R. Manson, J.P. Toennies, and Ch. Wöll, J. Chem. Phys. **86**, 7194 (1987).
[16] C.W. Skorupka and J.R. Manson, Phys. Rev. B **41**, 9783 (1990).
[17] *CRC Handbook of Chemistry and Physics*, 52nd ed., edited by R.C. Weast (Chemical Rubber Co., Cleveland, 1971), p. D-142.
[18] A. Reichmuth, Ph.D. thesis, Cambridge University, 1995.
[19] E. Hulpke, J. Lower, and A. Reichmuth, Phys. Rev. B **53**, 13 901 (1996).
[20] See, e.g., J.R. Manson, in *Helium Atom Scattering from Surfaces*, edited by E. Hulpke, Springer Series in Surface Sciences Vol. 27 (Springer, Berlin, 1992), p. 173ff.
[21] G. Benedek, N.S. Luo, P. Ruggerone, A. Reichmuth, and J.P. Toennies, Mater. Sci. Eng. B **23**, 123 (1994).
[22] See F. Hofmann, J.P. Toennies, and J.R. Manson, J. Chem. Phys. **101**, 10 155 (1994).
[23] D. Fuhrmann, Diplom thesis, Göttingen, 1995 (unpublished).
[24] A. Reichmuth, A.P. Graham, H.G. Bullman, W. Allison, and G.E. Rhead, Surf. Sci. **307-309**, 34 (1995).
[25] J.R. Manson, Phys. Rev. B **43**, 6924 (1991).
[26] D. Eichenauer and J.P. Toennies, J. Chem. Phys. **85**, 532 (1986).
[27] G. Comsa, Surf. Sci. **81**, 57 (1979).
[28] P.H. Dederichs, H. Schober, and D.J. Sellmeyer, in *Numerical Data and Functional Relationships in Science and Technology*, edited by K.-H. Hellwege and J.L. Olsen, Landolt-Börnstein, New Series, Group III, Vol. 13, Pt. a (Springer, Berlin, 1981), p. 69.